applied sciences

MDPI

*Article*

# Design and Evaluation of Flexible Support Based on Space Mirror

**Zhongyao Zhu [1], Ailing Tian [*,1], Bingcai Liu [1], Yongkun Wu [2] and Suotao Dong [2]**

[1] School of Opto-electronical Engineering, Xi 'an Technological University, Xi 'an, 710021, China;
[2] Zhongshan Institute of Changchun University of Science and Technology, Zhongshan 528437, China;
[*] Correspondence: ailintian@xatu.edu.cn.

**Abstract:** The mirror component is one of the most critical components in the space remote sensing payload, and the performance of its support essentially determines the imaging quality of the system. Mirror component need to have high face shape accuracy, high reliability and high stability. In this paper, taking the square mirror with the size of 550mm × 450mm as an example, we choose the Ultra-low expansion glass as the mirror blank material, and through in-depth research on the principle of the three-point backside support and the engineering realization, we design a three-point backside flexible support structure applied to the space mirror component. The design results are verified by simulation analysis, which shows that the weight of the mirror is 13.2 kg and the surface density can reach 48.5 kg/m$^2$. Under the effect of gravity acceleration of 1 g, within the range of temperature change from 16℃ to 24℃, bearing a forced displacement of 5 μm, the RMS value of the mirror component can reach 1/55$\lambda$ ($\lambda$ = 632.8 nm), which meets the demand of high face shape accuracy of the mirror component in space. Finally, the mechanical test was carried out on the assembled mirror component, the intrinsic frequencies of three directions of the mirror component were obtained through the test : 173.8 Hz, 176.4 Hz and 271.5 Hz, respectively, the changes of the mirror and its support structure were all less than 5″ after the 8g sinusoidal vibration test and the 5.66 g random vibration test, which indicates that the flexible support structure meets the requirements of the high reliability of the space remote sensing loads and the high accuracy of the space mirror component. It shows that the flexible support structure meets the high reliability and high stability requirements of space remote sensing loads. The theoretical data and test results in this research can provide theoretical references for mirror component of the same size and type.

**Keywords:** square mirror; flexible support; simulation analysis

**Citation:** Zhu, Z.; Yang, J.; Tian, A.; Liu, B.; Wu, Y.; Dong, S. Design and Evaluation of Flexible Support Based on Space Mirror **2023**, *12*, x. https://doi.org/10.3390/xxxxx

Academic Editor(s):

Received: date
Revised: date
Accepted: date
Published: date

**Copyright:** © 2023 by the authors. Submitted for possible open access publication under the terms and conditions of the Creative Commons Attribution (CC BY) license (https://creativecommons.org/licenses/by/4.0/).

## 1. Introduction

Nowadays, space remote sensing payload has entered a stage of rapid development, which puts forward higher and higher requirements for resolution of itself, while increasing the focal length and throughput aperture of the optical system are an effective way to improve the resolution of the ground image element. Therefore, in recent years, long focal length and large aperture have become the development trend of space remote sensing payload, and consequently, the ratio of mirror area and perimeter are getting larger and larger, the design of the mirror component becomes the most core of restricting the development of space remote sensing payload, and it is also one of the most urgent problems that need to be changed [1].

In the space field, two types of support for mirrors are mostly used: peripheral support and backside multi-point support. The peripheral support presses the mirror into the frame through the pressure plate, and the mirror is fixed with adhesive around the mirror. This form of support is simple and convenient, and is generally applicable to small-diameter mirrors. For medium and large-diameter mirrors with diameters larger than 350mm,

peripheral support will increase the structural size on the one hand, which is not conducive to the lightweight and small-sized design of space remote sensing loads, and on the other hand, it is also difficult to obtain high face shape accuracy. Backside multi-point support is to connect the back of the mirror with the support structure through appropriate connection methods. Compared with the peripheral support type, the backside multi-point support is easier to obtain higher surface shape accuracy, so the backside multi-point support is often used for medium and large aperture mirrors [2-3].

With the backside multi-point support mirror component, the mirror and support structure need to have good stiffness to cope with the large number of mechanical vibrations brought about by the transportation during the launch phase. At the same time, the mirror and support structure also need to have a lighter weight and better thermal unloading capability to cope with the complex and variable temperature environment during the on-orbit operation. It is theoretically contradictory to have both strong stiffness, light weight and flexible temperature unloading structure. Therefore, how to find a balance and a compromise among the contradictions, so that the index of the mirror component can reach an optimal solution, which becomes the key to the design of the support structure of the mirror component.

The object of this paper is the secondary mirror component in an optical system, which is at the farthest end of the system and needs to withstand a higher mechanical environment and a wider thermal environment than other components, and the surface shape of the secondary mirror will affect the imaging quality of the whole system. As the most remote optical glass component needs to have a low weight, the optical component needs to have a very high surface stability when subjected to a wide range of temperature variations, and needs to have a very high structural stability when subjected to a large order of magnitude of the mechanical environment [6]. However, light weight, high stiffness, and thermal stability are usually mutual constraint, a reasonable design is to seek a delicate balance in the contradiction, so that its technical parameters meet the requirements of use.

Detailed descriptions are given in this paper in terms of the selection of mirror materials, the layout of the support points of the mirror, and the design of the flexible support structure, with lighter weight, higher stiffness, and more stable face shape accuracy as the primary objectives. Using the finite element simulation with the actual engineering boundary conditions to analyze the designed mirror component, the design has been optimized several times based on the analysis results, and finally an optimal solution has been obtained. After loading and adjusting the mirror assembly, a series of environmental tests of small-scale sinusoidal scanning, sinusoidal vibration, and random vibration have been carried out, and after analyzing the test data, it is concluded that the design of the mirror component in this paper meets the requirements for the use of remote sensing payload in space.

## 2. Design of space mirror

### *2.1. Selection of Mirror Material*

Currently, the materials that can be used as mirror blanks for space mirrors are: fused silicon [7]: Zerodur, Silicon carbide, Beryllium and Ultra-low-expansion (ULE), The material parameters are shown in Table 1.

From Table 1, it can be seen that the ultra-low-expansion glass thermal expansion coefficient tends to be close to zero from 5°C to 35°C. From the material science aspect, the ultra-low-expansion glass belongs to the titanium dioxide-silicate glass, which has the property of being easy to be fused, allowing the optical component to have more processing possibilities, as well as to reduce its own weight [8-10].

The base structure design of the mirror follows the basis of ensuring rigidity and face shape accuracy, reducing weight, and possessing stress release capability. According to the characteristics of easy fusion bonding of ULE , the mirror is designed as three parts:

top mirror, middle mirror and bottom mirror, which are combined together by means of fusion bonding, as shown in Fig. 1.

Table .1 Comparison of mirror material parameters

| Material | Density g/cm$^3$ | Coefficient of linear expansion $\alpha$×10$^{-6}$/K | Modulus of elasticity Gpa |
|---|---|---|---|
| Fused silicon | 2.2 | 0.55 | 67 |
| Zerodur | 2.53 | 0.05 | 91 |
| Be | 1.87 | 11.3 | 287 |
| Sic | 3.12 | 2.24 | 400 |
| ULE | 2.21 | 0.03 | 68 |

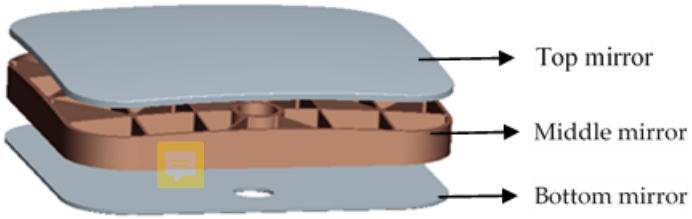



Fig.1 Schematic diagram of mirror blank

*2.2. Design of mirror configuration*

The force point of a mirror is related to the number of support points. For circular mirrors, Hall et al. proposed an empirical formula for calculating the number of support points of mirror. However, there is no reasonable and feasible formula for square mirrors. In this research, we take the outer circle of the square mirror as the maximum outer envelope size, bring it into the formula proposed by Hall et al. to get the approximate number of support points, and then optimize it through the later finite element simulation analysis.

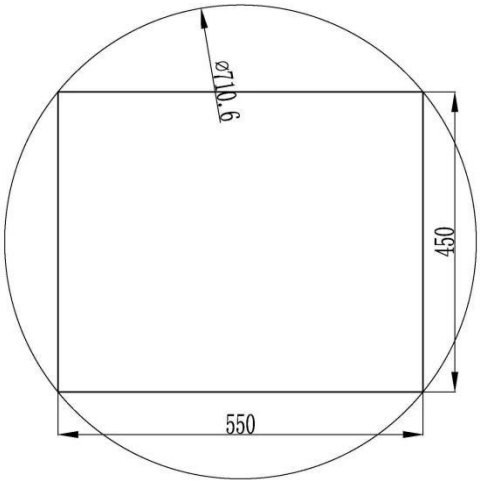



Fig.2 Schematic diagram of the external circle of the mirror

In this research, the size of the mirror is 550mm×450mm, as shown in the figure 2, and the diameter of its outer circle is 711mm, and the system index requires that the root-mean-square (RMS) of the back shape of the mirror's gravity change needs to satisfy the requirements of $\lambda/100$ ($\lambda$=632.8nm), which is calculated according to the following equation：

$$N = \frac{1.5r^2}{t}\sqrt{\frac{\rho g}{\delta E}} \quad (1)$$

In the equation, r is the radius, t is the height, ϱ is the material density, g is the gravitational acceleration, E is the modulus of elasticit, δ is the maximum self-weight deformation. Calculated from equation (2), the number of support points of a Φ711mm circular mirror is N=3.8. For a mirror in space, each support point has six degrees of freedom, translational movement along the X, Y, and Z directions, rotation around the X, Y, and Z coordinate axes, and the object is unable to produce relative movement after we have completely restricted all six degrees of freedom of all the support points. For space shape, triangular is the most stable compared with other shapes, so three-point support is chosen for small and medium diameter (≤Φ350mm) optical elements, while three-point or multiples of three are used to complete the support design for large diameter (≥Φ350mm) optical elements. In this paper, the number of support points based on the calculation is 3.8, so the three-point support design is chosen.

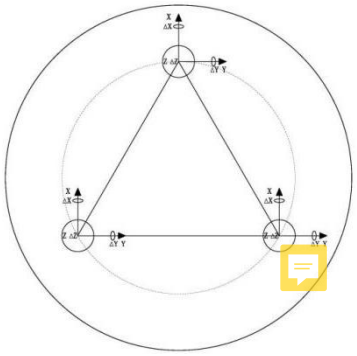


Fig.3 Mirror gravity load

*2.3. Design of mirror stiffener*

The stiffener structure is the key part of the mirror itself to release the stresses, and it is also the core of adapting to the large-span temperature-variable environment. The main components of stiffener configuration include: the thickness of the outer ring, the width, length and thickness of the stiffener.

At present, optical processing can be achieved in the form of lightweight reinforcement: triangular stiffener structure, square stiffener structure, hexagonal stiffener structure [16] (Figure 3). Stiffener structure form should not only take into account the weight of the mirror itself but also take into account its own stiffness, ease of production and achievability, finite element simulation analysis in the modal analysis, can characterize the strength of the structural stiffness, the greater the value of its calculation means that the stronger its own stiffness.

| Shape of stiffener | Weight | Mirror frequency |
|---|---|---|
| triangular stiffener structure | 13.2 kg | 1267.5 Hz |
| square stiffener structure | 13.5kg | 1225.6Hz |
| hexagonal stiffener structure | 13.7 kg | 1239.8 Hz |

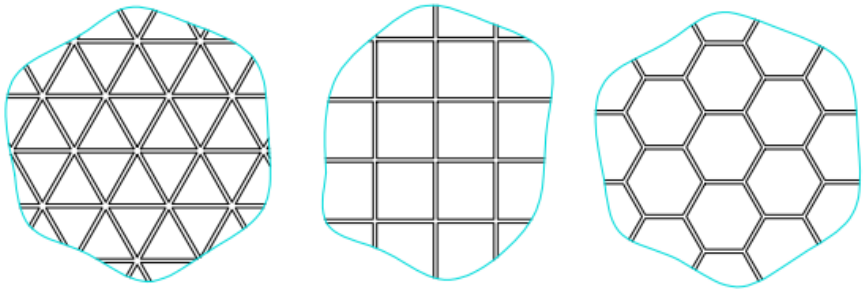


Fig.4 Honeycomb grid structure form

In this paper, the simulation models of three kinds of mirrors with the same thickness of stiffeners ( Tentatively 4mm ) are established and the modal analysis is carried out. As shown in Table 2, the modal and weight of different types of stiffener mirrors are obtained. Among them, the triangular stiffener structure has the highest mode and the lightest weight, which indicates that the reflector in this size range is more stable using the triangular stiffener structure. Therefore, this paper chooses the triangular stiffener structure.

Table 2 Comparative analysis of lightweight structure of sandwich

## 3. Design of support structure for space mirror component

### *3.1. Design of support structure*

In this study, the secondary mirror of a system is required to withstand the severe mechanical environment and a wide range of temperature change environment, which requires the mirror component not only to have a high degree of rigidity at the same time, but also need to have a relatively flexible component support structure to offload the temperature change. Firstly, a back three-point support structure is selected, and a new biaxial circular arc flexible hinge support structure is introduced on the basis of ensuring the stiffness of each component.

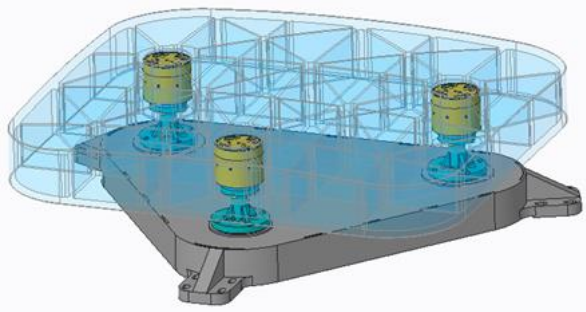


Fig 5 Schematic diagram of mirror component

The mirror component consists of mirror blank, nesting, flexible hinges, support seat and base plate as shown in Figure 5. First, the material of the mirror blank is determined to be ultra-low expansion glass. Considering the matching of the thermal properties of the material, the inlays connecting the support holes at the back of the mirror and the support structure are selected to be invar steel (4J32) with a lower coefficient of linear expansion, to reduce the effect of the temperature-varying environment on the mirror surface. Nesting, flexible hinges and support seat are screwed to each other. High specific stiffness, high strength, low density and mature processing of titanium (Tc4R) is selected for the flexible hinges and supports, while the base plate is made of carbon fiber composite material with high specific stiffness and low coefficient of linear expansion. The material properties are shown in the Table 3.

Table 3 Mirror material parameters

| Material | Density g/cm$^3$ | Coefficient of linear expansion $\alpha\times10^{-6}$/K | Modulus of elasticity Gpa | Poisson |
|---|---|---|---|---|
| ULE | 2.21 | 0.03 | 67.6 | 0.17 |
| TC4R | 4.45 | 9.1 | 110 | 0.34 |
| Invar Steel （4J32） | 8.18 | 0.05 | 145 | 0.25 |
| AlSiC | 2.9 | 9.8 | 145 | 0.32 |
| Optical cement | 1.7 | 110 | 600 | 0.49 |

*3.2. Design of flexible hinge*

Flexible hinges play a role in the whole support structure to protect the top and stabilize the bottom, it is necessary to have a certain degree of rigidity to ensure that the components can withstand the harsh mechanical environment, but also need to have a certain degree of flexibility to adapt to a wide range of temperature change environment, in order to find a point of agreement in the contradictory conditions, need to find a compromise value through the formula calculation and simulation analysis.

The new biaxial circular arc flexible hinges support structure designed in this paper is such that each supporting point provides two degrees of freedom in the optical axis direction and tangential direction, and the three supporting points provide exactly six degrees of freedom (three axial supports constrain axial movement, radial rotation, and tangential rotation; three tangential supports constrain tangential movement, radial movement, and axial rotation), which realize decoupling of the degrees of freedom, and this is

the typical Boise kinematic localization support. This support structure restricts the rigid motion of the mirror, and it can isolate the mirror from the elastic deformation of the surroundings, thus effectively protecting the mirror [10].

Analyze and calculate the flexible hinge deflection and corner [11] of the flexible hinge support structure. The empirical equations for the flexible hinge deflection y and corner θ are shown below:

$$y = \int [\int \frac{12R\sin\alpha M(x)}{Eb\left(2R+\tau-2R\sin\alpha\right)^3} d\alpha] da \quad , \tag{2}$$

$$\theta = \int \frac{12R\sin\alpha M(x)}{Eb\left(2R+\tau-2R\sin\alpha\right)^3} d\alpha \quad , \tag{3}$$

In the equations, R is the cutting radius of the hinge, τ is the thinnest part of the thickness of the hinge, b is the width of the hinge, and M(x) is the torque applied to the end of the hinge, which can be considered as a constant.

Numerical integration method can be used to obtain the value of corner stiffness of flexible hinge under different values of R and τ, and then carry out curve fitting, the results can be found that the corner stiffness increases with the increase of τ value, and the corner stiffness is not sensitive to the change of R value, so in the process of flexible hinge parameter selecting, the value should be set according to the structural dimensions and technological requirements, then adjust the value of t until the mirror ultimately meets the requirements of stiffness, strength and thermal dimensional stability requirements. According to the above equations, the R value of the flexible hinge in this paper is 4 mm, and the τ value is 3.5 mm. The design model of the flexible hinge is shown in Fig. 6.

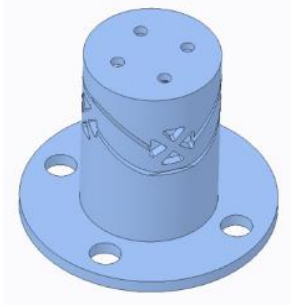


Fig 6 Schematic diagram of flexible hinge model

## 4. Analysis and evaluation

The key factor of the imaging quality of space remote sensing payload depends on the surface shape of the mirror component, and the main factor affecting the surface shape of the mirror is the stiffness of the component composed of a number of materials and the thermal matching of the combination of various materials, the material data of each part of the mirror component are provided in Table 3. The numerical value will be given to each component of the simulation model after mechanical and thermal coupling analysis, according to the results of the analysis to determine the rationality of the design.

The simulation analysis of the mirror component selects the tetrahedral mesh, which can divide any complex model, quickly and automatically form. In the key area, it is easy to use the curvature and approximate size function to automatically refine the local mesh, which can greatly save the time of meshing.

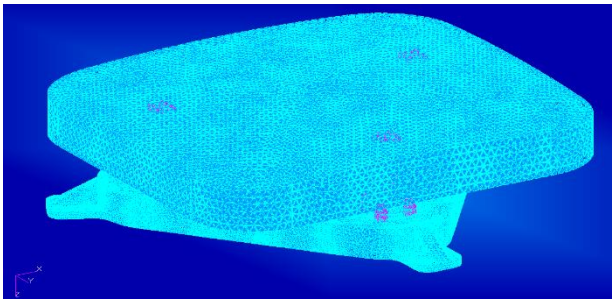


Fig. 7 Finite element model of mirror component

*4.1. Modal analysis*

Modal analysis is an important parameter in the initial evaluation of design rationality, and its analysis results can objectively reflect the mechanical characteristics of the structure and characterize the vibration response of the structure under mechanical load.

Modal analysis theory is a technique applied to determine the vibration characteristics of a structure, by which mass frequencies, vibration and mode-participation coefficients can be determined [17-18]. Performing a modal analysis at the beginning of the design allows the structure to avoid resonating or vibrating at a specific frequency, allows the designer to find out how the structure responds to different types of dynamic loads earlier stage, helps to estimate and solve the control parameters in other dynamic analyses.

By obtaining the fundamental frequency of the structure before the component is machined, and then optimizing the design, to ensure that it avoids forced vibrations during launch and transportation, avoiding the occurrence of resonance phenomena which could damage the structure.

By simulation, the first four order modes of the overall mirror components are shown in Table 4 and the analysis results are shown in Table 5. From the simulation results, it can be concluded that the first-order modal of the mirror components is 179.6 Hz, which has a higher stiffness compared with the mirror components of the same size.

Table 4 Four vibration modes of the mirror component

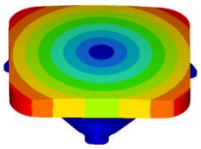
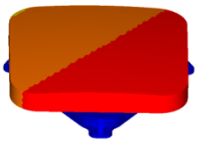
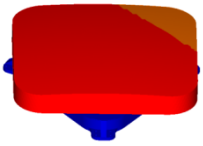
| First order of vibration modes | Second order of vibration modes |
|---|---|
|  |  |
| **Third order of vibration modes** | **Fourth order of vibration modes** |
|  |  |

Table 5 Results of four modes analysis of the mirror component

| Order | Frequency (Hz) | Vibration modes description |
|---|---|---|
| 1 | 179.6 | Main mirror rotates around Z-axis |
| 2 | 188.1 | Main mirror translational movement towards X-axis |

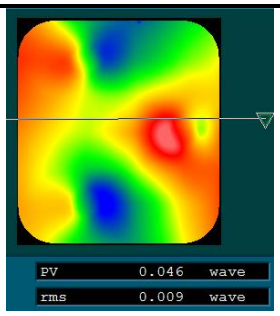
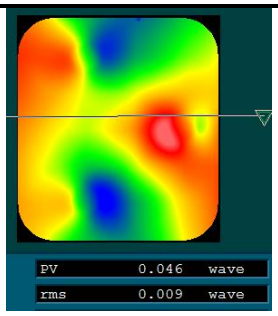
| | | |
|---|---|---|
| 3 | 215.4 | Main mirror translational movement towards Y-axis |
| 4 | 303.7 | Main mirror rotates around Y-axis |

*4.2. Gravity load analysis*

During the ground mounting process of the mirror component, the mirror will be affected by gravity, the degree of its influence will be analyzed by simulation during the component design process and appropriate countermeasures will be taken [19-20].

The coordinate values of all points on the mirror surface are obtained by simulation analysis and brought into MATLAB calculation to simulate the mirror surface shape. As shown in the table below, it is the root-mean-square (RMS) value of the surface shape of the mirror component after loading the gravity in X and Y directions through simulation analysis (since the Z direction is the vertical direction of the optical axis, not the direction of loading and adjusting, the mirror component is not affected by gravity in the stage of on-orbit operation, therefore, it is not included in the scope of the analysis).

Table 6 RMS of mirror shape error under different environments

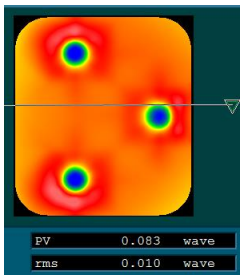
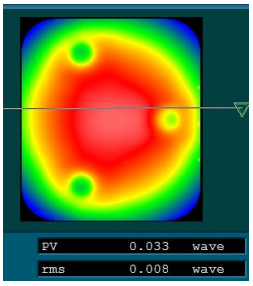
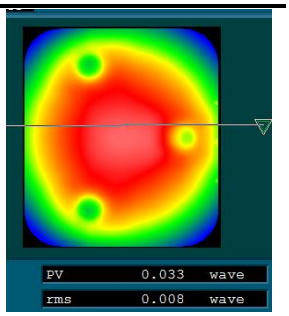
| Working condition | X Gravity load (1G) | Y Gravity load (1G) |
|---|---|---|
| Surface error RMS/λ (λ=632.8nm) |  X：RMS=0.009λ |  Y：RMS=0.009λ |

*4.3. Temperature load analysis*

Mirror component works in the track process, the mirror component will be affected by the temperature change of environment, in the process of component design, through simulation to analyze the degree of its impact, and make the corresponding countermeasures [19-20]. According to the temperature range given by the thermal control analysts, loading temperature conditions on the mirror assembly, in this paper, the mirror component loading temperature load for 16 ℃ ~ 24 ℃, the mirror component axial and radial affected by the temperature will show different characteristics, need to load the mirror component axial, radial 4 ℃ temperature gradient load. The coordinate values of all the points on the mirror surface are obtained by simulation and analysis software, which are brought into MATLAB calculation to simulate the mirror surface shape. As shown in Table 7, it is the root mean square value of the surface shape of the mirror component after loading the temperature load by simulation analysis.

Table7 RMS of mirror shape error under different environments

| Working condition | Temperature load (20±4℃) | Axial temperature gradient load (4℃) | Radial temperature gradient load (4℃) |
|---|---|---|---|

| | | | |
|---|---|---|---|
| Surface error RMS/λ (λ=632.8nm) |  |  |  |
| | RMS=0.01λ | RMS=0.008λ | RMS=0.008λ |

*4.4. Forced displacement analysis*

Mirror component in the ground mounting process, the parts and parts assembly contact surface can not reach the ideal fitting, the surface to surface fit will cause relative displacement, which can be directly or indirectly transmitted to the mirror to cause changes in the mirror surface shape, we usually refer to this influence factor as the forced displacement. Analyze the degree of impact through simulation in the component design process and make corresponding countermeasures [19-20]. According to the support structure of the mirror component designed in this paper, there are two contact points that will produce forced displacement, which are the contact surface between the support base and the base plate, and the contact surface between the base plate and the other structures, as shown in the figure below, at this stage, the contact surface error can be considered to be 5μm.

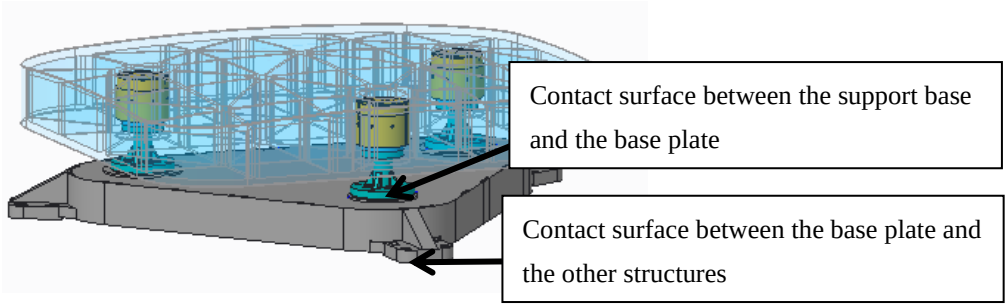
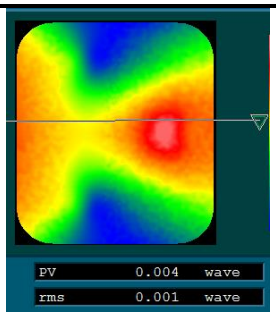
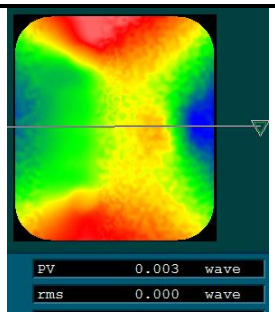



Fig 8 Schematic of forced displacement contact surface

The variation of coordinates of all points on the mirror surface are obtained by the simulation and analysis software, which are brought into MATLAB calculations to simulate the values of the face shape. As shown in Table 8, the following is the root mean square value of the face shape of the mirror component after undergoing forced displacement obtained through simulation analysis.

Table 8 RMS of mirror shape error under different environments

| Working condition | Forced displacement (5μm) | Forced displacement (5μm) |
|---|---|---|
| Surface error RMS/λ (λ=632.8nm) |  |  |
| | RMS=0.001λ | RMS=0.0005λ |

*4.5. Error analysis*

After completing the simulation analysis and calculation of 1 g gravity load, forced displacement (5 μm) load, 16°C~24°C temperature load, axial gradient 2°C load, and radial gradient 2°C load, the data results in Tables 8, 9, and 10 are substituted into Eq. (3) to obtain the average value of RMS for the surface shape of the mirror component.

$$\begin{aligned}&\sqrt{X^2+Y^2+t^2_{(20\pm2^\circ)}+S^2_{(forced\ displacement)}+t^2_{(axial\ or\ radial\ 2\ ℃)}} \\ &=\sqrt{0.009^2+0.009^2+0.01^2+0.001^2+0.008^2} \\ &=0.018\lambda\end{aligned} \tag{3}$$

The average value of the root mean square of mirror shape is calculated to be 0.018$\lambda$.

*4.6. Mechanical tests*

The space remote sensing payload will experience a short mechanical environment during the launch phase [21], in order to guarantee the stability of the mirror component during the on-orbit operation phase, mechanical tests are required for the component during the ground phase, including small-scale feature-level sinusoidal scanning test, sinusoidal vibration test and random vibration test.

During the mechanical test, it is necessary to paste two test signal points on the mirror component, which are placed at the center of the mirror and at the center of the base. The test signal points can be used to monitor the changes of the participating products in the mechanical test through the data in the software during the mechanical test, and at the same time, after the end of the mechanical test, through the computation of all the data, we can find out the location of the component's weak position and the specific value. Two control signal points are pasted at the edge position of the vibration tooling to control the excitation of the mechanical test. By obtaining the numerical changes of the test points, it can be judged whether the designed component can withstand the influence brought by the mechanics.

The tests procedure in this paper start with a small-scale feature-level sinusoidal scanning tests with frequency between 10 and 500Hz and excitation of 0.2g, followed by an 8g sinusoidal vibration test with frequency between 0 and 100Hz and excitation of 8g, then a feature-level sinusoidal scanning test with frequency between 10 and 500Hz and excitation of 0.2g, followed by a random vibration test ( 2 minutes ) with frequency between 20 and 2000Hz and excitation of 5.66grms random vibration test ( 2 minutes ), and finally carry out the frequency between 10~500Hz, the excitation is 0.2g feature level sinusoidal scanning test. During the test preparation stage, firstly, connect the vibration tooling with the shaking table, then connect the mirror component with the vibration tooling, finally, paste the test points and control points, the schematic diagram for the mechanical tests of the mirror component are shown as follows.

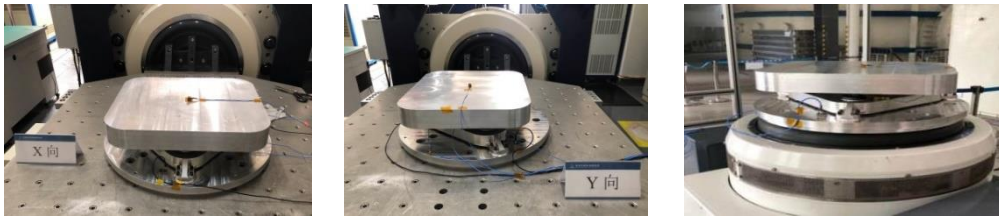



Fig. 9 Mechanical test diagram of mirror component

*4.7. System evaluation*

*4.7.1 Comparison of small-scale feature level sinusoidal scanning tests*

After collating and comparing the results of three small-scale feature level scanning tests, as shown in the table below, it is possible to obtain the resonance frequency of each measurement point of the mirror component, so that the intrinsic frequency of the component can be obtained. As shown in the table below, the final results show that the intrinsic frequency of the mirror component in the X direction is 173.8 Hz, the intrinsic frequency of the mirror component in the Y direction is 176.4 Hz, and the intrinsic frequency of the mirror component in the Z direction is 271.5 Hz. The simulation result is 179.6 Hz, and the error with the real test result is 5.8Hz, which meets the requirement of analyzing accuracy, and verifies the validity of the finite element model.

Table 9 Comparison of mirror component intrinsic frequencies

| Direction | First time | Second time | Third time | Magnitude of change |
|---|---|---|---|---|
| X | 178.6Hz | 176.4Hz | 173.8 Hz | 4.8 Hz |
| Y | 177.9Hz | 177.3Hz | 176.4Hz | 1.5 Hz |
| Z | 273.1Hz | 272.7Hz | 271.5Hz | 1.6 Hz |

After three times small-scale feature-level scanning tests, the intrinsic frequency of the mirror component varies by 4.8 Hz, 1.5Hz and 1.6 Hz in X, Y and Z directions, and the frequency deviation is less than 5%, which shows that the component has good stiffness and little variation before and after the test.

*4.7.2 Comparison of sinusoidal vibration tests*

After the mirror component has been subjected to sinusoidal vibration tests in X, Y and Z directions, the values of the two test points of the mirror component are not enlarged between the frequencies of 0 and 100 Hz, as shown in the figure below, which indicates that the mirror component can withstand sinusoidal vibration of this magnitude.

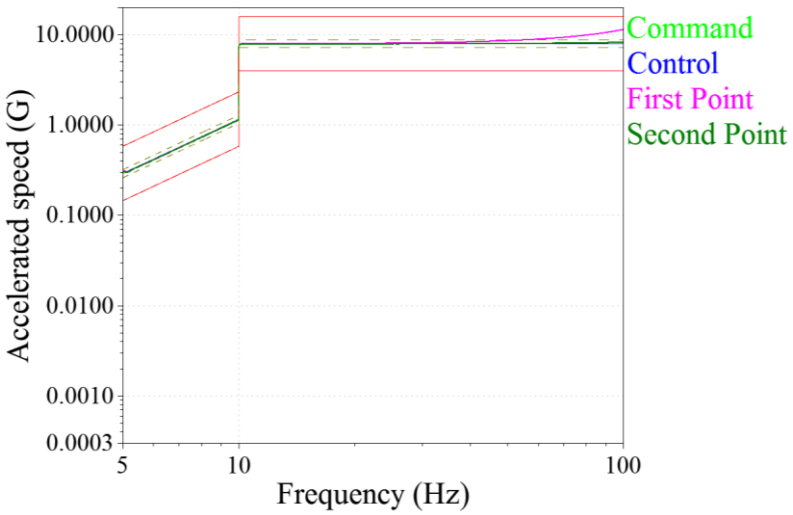



Fig. 10 Schematic diagram of sinusoidal vibration test curve of mirror component

*4.7.3 Comparison of random vibration tests*

After the mirror component has been subjected to random vibration tests in the X, Y and Z directions, the following table shows the comparison of the data of the mirror component in random vibration, through which it can be seen that in the random vibration of the mirror component in the X, Y and Z directions, the position of the largest response amplification is located in the center of the base, and the magnification of the response is

controlled to be less than 5 times. It shows that the mirror component can withstand sinusoidal vibration of this magnitude, at the same time, it proves that the stiffness of the component can overcome the influence brought by the mechanics of the launching stage.

Table 10 Comparison of random vibration data for mirror component

| Direction of vibration | POV | RMS of total response (grms) | Response amplification |
|---|---|---|---|
| X | Input | 5.677 | |
| | Mirror center | 16.91 | 2.97 |
| | Base center | 20.16 | 3.55 |
| Y | Input | 5.677 | |
| | Mirror center | 19.86 | 3.49 |
| | Base center | 22.4 | 3.94 |
| Z | Input | 5.677 | |
| | Mirror center | 18.68 | 3.29 |
| | Base center | 21.15 | 3.72 |

*4.7.4. Comparison of displacement change data*

The mirror component is equipped with 2 optical cubic mirrors of 13 mm × 13 mm × 13 mm, which are used to test the positional change of the structural member relative to the optical member before and after the mechanical test. As shown in the figure, one optical cubic mirror is affixed to the edge of the mirror and another is affixed to the edge of the base, which are used to test the angular change between the 2 reference mirrors before and after the mechanical test.

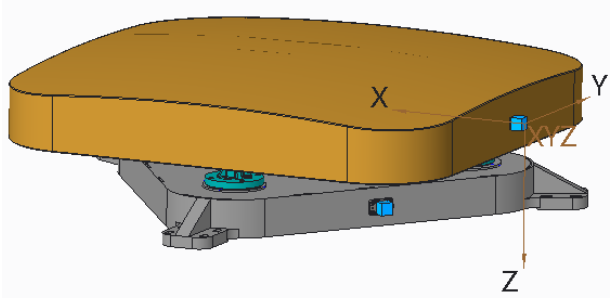



Fig 11 Schematic of optical cubic mirror position

After three small-scale feature level scanning tests, one sinusoidal vibration test, and one random vibration test, the angular changes in the X, Y, and Z directions of the mirror and the base are 5.678872″, -4.180947″, and -5.87815″. As shown in the table below, the optical cubic mirror test results show that the changes between the mirror and the support structure before and after the mechanical test are less than 5″, indicating that there is no relative movement between the mirror and the support structure before and after going through the mechanical test, which further proves that the flexible support structure in this paper can withstand the harsh mechanical environment.

Table 11 Variations before and after the mechanical test

| Variations △ before and after the mechanical test (″) |
|---|

| | Mirror (X, Y, Z) | | |
|---|---|---|---|
| Structure (X, Y, Z) | 5.678872 | -7.386751 | -23.4734 |
| | 3.457164 | -4.180947 | -6.37103 |
| | 23.51495 | 6.529278 | -5.87815 |

## 5. Conclusions

To ensure that the space remote sensing load can work normally in the orbit operation stage, the mirror component not only needs to have high face shape precision, but also needs to maintain the stable adaptability of the overall structure after withstanding high mechanical changes and wide temperature span, which are the fundamental of the design for the environmental space remote sensing payload. Aiming at the research background of the square mirror in the optical system, this paper takes the lightweight design of the mirror as the premise, uses ultra-low expansion glass as the optical raw material of the mirror, gives full play to the characteristics of the material's welding, designs the mirror as a three-layer sandwich structure, and chooses the triangular stiffener in the middle layer. In this design, the local stiffness of the mirror is enhanced while the lightweight design is achieved; A biaxial circular arc flexible hinge support structure is innovatively proposed to strengthen the structural rigidity while offloading the effect of temperature on the mirror component; using the simulation analysis method, a simulation model similar to the actual optical component is established, and its static mechanics, temperature field, and part-to-part forced displacement are analyzed and calculated. The results show that the RMS value of the face shape of the mirror component reaches 0.0009$\lambda$ ($\lambda$ = 632.8 nm) under the effect of 1 g gravity, 0.01$\lambda$ ($\lambda$ = 632.8 nm) within the temperature-variable environment from 16°C to 24°C, and 0.001$\lambda$ ($\lambda$ = 632.8 nm) under the effect of 5 μm forcing displacement. Finally, using the mechanical tests to verify the component, from the test data, the component in the X, Y, Z three directions of the intrinsic frequency are 173.8 Hz, 176.4 Hz, 271.5 Hz, close to the results of the simulation calculations of 179.6 Hz; Optical tests are added before and after the mechanical tests, and the results show that the variation of the mirror and the support structure in the X, Y, and Z directions is less than 5″, which further proves the reliability of the simulation and analysis results. The flexible support design of the square reflector studied in this paper has the static and dynamic stiffness to withstand the mechanics of the launch section and the stability to adapt to the thermal dimension after orbit. It shows that the design is reasonable and reliable for space environment adaptability. At the same time, the design and test verification methods of the flexible support of the square mirror can provide certain reference for the design and test of similar space mirrors, and can also provide technical guidance for the relevant research of professionals in the industry.

**Author Contributions:** Conceptualization, Z.Z. and S.D.; methodology, Z.Z.; software, S.D.; validation, J.Y., S.D. and A.T.; formal analysis, Z.Z.; investigation, B.L.; resources, S.D.; data curation, Z.Z.; writing—original draft preparation, S.D.; writing—review and editing, Y.K.; visualization, S.D.; supervision, X.Z.; project administration, S.D.; funding acquisition, Y.K. All authors have read and agreed to the published version of the manuscript.

**Funding:** Not applicable.

**Institutional Review Board Statement:** Not applicable.

**Informed Consent Statement:** Not applicable.

**Data Availability Statement:** The data used in this research is available from the corresponding author upon reasonable request.

**Conflicts of Interest:** Not applicable.

## Reference


1. STAHL H P,POSTMAN M,MOSIER G,et a1..AMTD:update of engineering specifications derived from science requirements for future UVOIR space telescopes[C].SPIE Astronomical Telescopes+Instrumentation. International Society for Opticsand Photonics,2014:91431T-91431T-8.
2. MILLER D W,DE WECK O L,MOSIER G E.Framework for multidisciplinary integrated model-ing and analysis of space telescopes[C].Workshopon Integrated Modeling of Telescopes.Interna-tional Society for Optics and Photonics,2002:1-18.
3. UEBELHART S A.Non-deterministic design andanalysis of parameterized optical structures dur-ing conceptual design[D].Massachusetts Instituteof Technology,2006.
4. Yan Chang Xiang,Xu Jie,Peng Ya.Stray light suppression of off-axis triple mirror space optical telescope systems[J].Optics andPrecision Engineering,20l0,18(2):289-293.
5. Matthias R K,Peter H.UItralightweightedHB-Cesic ©one-meter mirror demonstrator[C].SPIE,2010,7739:77392K-1-8.
6. ZHANG X J.Space telescope aspherical mirror structure design based on SiC material[J].Infra- red and Laser Engineering.2007,36(5):577-582.(in Chinese)
7. BaoHe,Li Zhilai.Design of the strip SiC mirror supporting structure and lightweight [J]. Optical Technique,2008,34(4):593-596.
8. STAHL H P.AdvancedMirrorTechnology Development for Very Large Space Telescopes[C]//American Astronomical SocietyMeeting. Baltimore,MD:American Astronomical Society Meeting Abstracts #223, 2011.
9. EGERMAN R, MATTHEWS G, WYNN J, etal. The Current and Future State-of-the-art Glass Optics[C]//Astro2010: TheAstronomy and Astrophysics Decadal Survey. 2009.
10. STAHL H P. Advanced Mirror Technology Development (AMTD) Project: Overview and Year FourAccomplishments[C]//SPIE Astronomical Telescopes + Instrumentation. Edinburgh, United Kingdom, 2016.
11. Bittner H, Erdmann M, Haberler P. SOFIA Primary Mirror Assembly: Structural Properties and Optical Performance[C]. Proceedings of SPIE 4857. 2003: 266-273.
12. PARKS R E.Engineering with lightweight mirrors[C]. Pro-ceedings of SPIE,1985,571.
13. ANDERSON D.Gravity denections of lightweighted mirrors[C]. Proceedings of SPIE,1982,332.
14. FRIEDMAN E.Photonjcs Rules of Thumb[M].New York:McGraw Hill,2003.
15. XU H, GUAN Y J. Structural design of 1 m diameterspace mirror component of space camera[J]. Optics andPrecision Engineering, 2013, 21(6): 1488-1495.
16. YANG J W,HUANG Q L.Optimized design of structure parameters for large aperture mirrors [J].Chinese Space Science and Technology,2011(4):77-83.(in Chinese)
17. Li Zhilai, Xu Hong, Guan Yingjun, et al. Structural design of1.5 m mirror subassembly for space camera [J]. Optics andPrecision Engineering, 2015, 23(6): 1635-1641. (in Chinese)
18. Zhang Bowen Wen,WangXiao Yong,Zhao Ye. Development of space-based large aperture mirror support technology[J]. Infrared and Laser Engineering,2018,47(11):1113001.(in Chinese)
19. Wu Qingwen, Yang Hongbo, Yang Jinsong, et al. Design and analysis for primary mirror and its support of space camera [ J ]. Optical Technique , 2004, 30 (2 ): 152 -156. (in Chinese)
20. Zhu Nengbing. Research on the design of the supporting structure of lightweight mirror [D]. Chengdu: University of Chinese Academy of Sciences, 2016. (in Chinese)
21. Wang Ke Jun,Dong Jin Hong.Composite support structure of large aperture mirror of space remote sensor[J].Optics andPrecision Engineering, 2016, 24(7): 1719-1730.